

Multiconformational Surfaces in Porphyrins: Previews into Excited-State Landscapes

K. M. Barkigia,[‡] D. J. Nurco,[†] M. W. Renner,[†] D. Melamed,[†] K. M. Smith,[‡] and J. Fajer^{*,†}*Department of Applied Science, Brookhaven National Laboratory, Upton, New York 11973, and Department of Chemistry, University of California, Davis, California 95616**Received: September 15, 1997; In Final Form: November 4, 1997[⊗]*

The crystal structures of four different conformers of the sterically encumbered porphyrins ZnDPP, H₂DPP, and NiDPP are reported (DPP = 2,3,5,7,8,10,12,13,15,17,18,20-dodecaphenylporphyrin). In combination with two previously published structures of H₂DPP and NiDPP, the crystallographic results illustrate the remarkable range of different conformational surfaces possible within a single family of compounds with the same peripheral substituents. These results establish that the multiple conformational landscapes inferred from the excited-state dynamics of the molecules already exist in the ground state and thus offer previews into the conformations that may also be accessible in excited states. Electron paramagnetic resonance (EPR) results for the ZnDPP and NiDPP π cation radicals indicate that the radicals retain a_{2u} spin-density profiles despite the extensive peripheral substitutions and the significant nonplanarity of the parent compounds.

Introduction

The introduction of multiple peripheral substituents in porphyrins affords facile synthetic avenues to new classes of chromophores with significantly altered optical, redox, ligation, radical, and excited-state properties that result from conformational distortions of the macrocycles.^{1–7} In turn, the nonplanar porphyrins begin to document and model the consequences of skeletal deformations increasingly seen in crystal structures of protein complexes comprised of porphyrinic chromophores⁸ and prosthetic groups.^{9,10}

In comparison to planar 5,10,15,20-tetraphenylporphyrins (TPP), the sterically encumbered, nonplanar zinc and free-base 2,3,5,7,8,10,12,13,15,17,18,20-dodecaphenylporphyrins (ZnDPP and H₂DPP) exhibit shortened lifetimes of the lowest excited singlet state, reduced fluorescence yields, and large Stokes shifts between their absorption and emission maxima. Results in several solvents indicate that the altered excited-state behaviors arise not from solvent interactions but rather from the ability of nonplanar molecules to traverse multiple conformational surfaces in the excited state.^{1a,2} Similar photoinduced conformational “surfing” is believed to control the $(\pi, \pi^*) \rightarrow (d, d) \rightarrow$ ground-state deactivation pathways in NiDPP.^{1b}

We present here X-ray structures of ZnDPP, H₂DPP, and NiDPP that illustrate the types and multiplicities of these conformational surfaces: ZnDPP adopts a true saddle conformation,¹¹ H₂DPP *two* different saddles, and NiDPP *three* different conformations that range between different degrees of ruffling¹¹ and a combination of ruffling and saddle. These results clearly demonstrate that the multiple conformations inferred from the excited state dynamics do indeed exist, are already accessible in the ground states and, thus, that they are separated by relatively small energy barriers^{4a,10} that facilitate surface crossings in the excited states.

In a related context, both out-of-plane distortions and

substitutions at the β pyrrole positions have been proposed to affect orbital occupancy and mixing of the a_{1u} and a_{2u} highest occupied molecular orbitals (HOMO and HOMO-1) in porphyrin π cation radicals.^{6,7,12,13} Such occupancies are particularly relevant to the long-standing interest in the electronic profiles and properties of the ferriyl π cation radicals observed in the catalytic cycles of peroxidases, catalases, and cytochromes P450, and of the many π cation radicals designed to mimic those bioreactions.^{12–14} EPR spectra of ZnDPP⁺·ClO₄[−] and NiDPP⁺·ClO₄[−] reported here indicate that these π radicals retain the a_{2u} spin profiles found in the simpler TPPs,¹³ notwithstanding the eight additional β phenyl substituents of the DPPs and the significant nonplanarity of their parent compounds.¹⁵

Methods

The syntheses of H₂DPP¹⁶ and metallo DPPs⁴ have been described previously. ZnDPP and NiDPP are readily oxidized to π cation radicals with AgClO₄ in CH₂Cl₂.⁵ Electron paramagnetic resonance (EPR) spectra of the radicals were recorded on a Bruker ESP 300E spectrometer. g -values (2.0027 for ZnDPP⁺·ClO₄[−] and 2.0068 for NiDPP⁺·ClO₄[−]) were referenced against the perylene radical.

Crystallography of ZnN₄C₉₂H₆₀·3.5(C₂Cl₃H) (ZnDPP). ZnDPP was crystallized from trichloroethylene/hexane in space group $Pm\bar{m}n$ with $a = 18.645(5)$ Å, $b = 28.619(11)$ Å, $c = 8.150(2)$ Å, $V = 4348.9(23)$ Å³, and $Z = 2$. Because of the small crystal size, $0.18 \times 0.05 \times 0.05$ mm, data were collected at beamline X7B of the Brookhaven National Synchrotron Light Source (NSLS) at 153 K with $\lambda = 0.956$ Å using imaging plates. A total of 17 153 reflections ($\pm h \pm k \pm l$) were recorded and reduced with DENZO/SCALEPAK to give 4540 unique reflections. The structure was solved with SIR92 and refined with SHELXL93 to $R1 = 0.064$, $wR2 = 0.176$ for $I > 2\sigma(I)$, and $R1 = 0.091$ and $wR2 = 0.200$ for all data. Additional details of the refinement and complete sets of coordinates, bond distances, and bond angles are included in the Supporting Information. A second form of ZnDPP with 5 solvate molecules of cyclohexane crystallized in space group $P4_2/nmc$. Refinement of data obtained at 130 K yielded parameters that agreed within

[†] Brookhaven National Laboratory.[‡] University of California.^{*} Address correspondence to this author. Fax: 516-344-3137. E-mail: fajerj@bnl.gov.[⊗] Abstract published in *Advance ACS Abstracts*, December 15, 1997.

3–4 σ with those of the ZnDPP in space group *Pmmn*. The data are also included in the Supporting Information.

Crystallography of $\text{H}_2\text{N}_4\text{C}_{92}\text{H}_{60}\cdot 3(\text{H}_2\text{O})$ (H_2DPP). H_2DPP was crystallized from wet alcoholic KOH in space group *Pnma* with $a = 14.945(4)$ Å, $b = 24.594(11)$ Å, $c = 24.403(11)$ Å, $V = 8465.5(62)$ Å³, and $Z = 4$. Data were collected at 200 K on an Enraf-Nonius CAD4 diffractometer with Cu K α radiation. A total of 5805 reflections ($+h+k+l$) were measured in the range $4 \leq 2\theta \leq 110^\circ$ with 5799 of them unique. The structure was solved with SIR88 and refined with SHELXL93 to $R1 = 0.172$, $wR2 = 0.337$ for $I > 2\sigma(I)$, and $R1 = 0.437$ and $wR2 = 0.592$ for 5780 data. The high R values result from the poor quality of the crystal. Nonetheless, the conformation of the molecule is unambiguous and esds range between 0.01 and 0.02 Å. Additional details are included in the Supporting Information.

Crystallography of $\text{NiN}_4\text{C}_{92}\text{H}_{60}$ (NiDPP). NiDPP was crystallized from difluorobenzene/pentane in space group *C222₁* with $a = 15.901(3)$ Å, $b = 16.324(4)$ Å, $c = 30.733(7)$ Å, $V = 7977.3(31)$ Å³, $Z = 4$. 3715 reflections ($+h+k+l$) were collected at 200 K on an Enraf-Nonius CAD4 diffractometer with Cu K α radiation in the range $4 \leq 2\theta \leq 130^\circ$. The structure was solved with SIR92 and refined with SHELXL93 to $R1 = 0.089$, $wR2 = 0.237$ for $I > 2\sigma(I)$, and $R1 = 0.126$ and $wR2 = 0.286$ for all data. A second data set was also collected at 298 K. Within the precisions of the determinations, the structures are identical at the two temperatures.

Crystallography of $\text{NiN}_4\text{C}_{92}\text{H}_{60}\cdot 3.5(\text{CCl}_3\text{H})$. NiDPP was crystallized from 2-propanol/chloroform in space group *P2₁2₁2₁* with $a = 17.275(3)$ Å, $b = 17.284(2)$ Å, $c = 28.155(4)$ Å, $V = 8406.6(21)$ Å³, and $Z = 4$. Data were collected at 130 K on a Siemens P4 diffractometer equipped with a Cu rotating anode. A total of 6833 reflections were measured in the range $6 \leq 2\theta \leq 112^\circ$. The structure was solved with SHELXS and refined with SHELXL93 to $R1 = 0.069$, $wR2 = 0.179$ for $I \geq 2\sigma(I)$, and $R1 = 0.076$, $wR2 = 0.207$ for 6783 reflections. A different solvate of NiDPP , $\text{NiN}_4\text{C}_{92}\text{H}_{60}\cdot 1.5(\text{H}_2\text{O})$ crystallized from (wet) methylene chloride/pentane in the same *P2₁2₁2₁* space group with $a = 17.343(4)$ Å, $b = 17.282(4)$ Å, $c = 26.783(7)$ Å, $V = 8027.4(34)$ Å³, and $Z = 4$. Aside from the solvent molecules, the structure does not differ from the other *P2₁2₁2₁* polymorph within the precisions of the refinements. Additional details for all the NiDPP structures are included in the Supporting Information.

Results

An edge-on-view of ZnDPP is shown in Figure 1. The molecule adopts a classic *S₄* saddle conformation¹¹ with the *meso* carbons nearly in the mean porphyrin plane and adjacent pyrrole rings alternately canted above and below that plane. The numerical deviations from planarity are presented in Figure 1: The absolute displacements of the pyrrole β carbons average 0.955 Å, while those of the *meso* carbons average only 0.01 Å. The phenyl rings at the *meso* positions form dihedral angles of 48° with the porphyrin plane. The two phenyl rings that flank them average angles of 59° with the same plane. Center-to-center distances between adjacent phenyls at the β positions average 4.54 Å; distances from the *meso* phenyls to their flanking β neighbors average 3.59 Å. Additional representative bond distances are listed in the Figure 1 legend. Complete sets of bond distances, angles, and coordinates are available in the Supporting Information.

A second crystal form of ZnDPP in space group *P4₂/nmc* with five solvate molecules of cyclohexane was also obtained

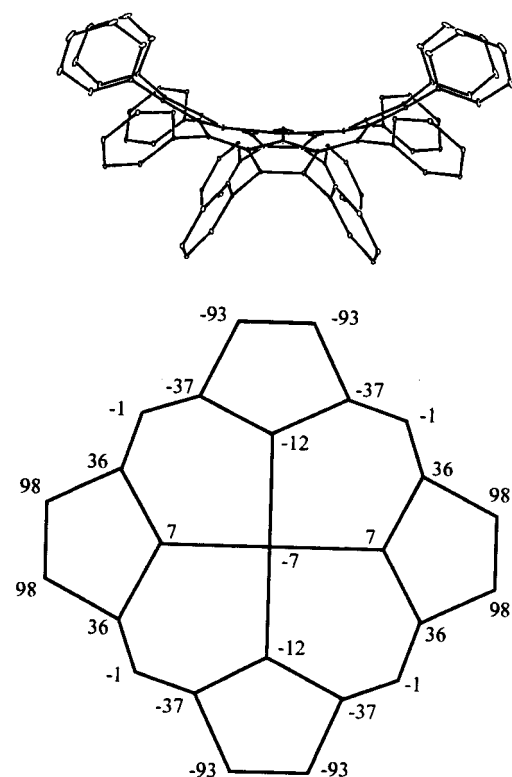


Figure 1. Top: Edge-on-view of ZnDPP. For clarity, the hydrogens are omitted and the thermal ellipsoids are reduced to enclose 1% probability. Bottom: Deviations of the atoms of the ZnDPP core from the 24-atom mean plane, in units of 0.01 Å. Note that the equivalent up and down displacements of the pyrrole rings form a saddle distortion. Representative bond distances, in Å: Zn–N = 2.037(4), N–C α = 1.376(3), C α –C β = 1.456(4), C β –C β = 1.371(6), C α –C meso = 1.412(4).

and yields a similar saddle distortion. At 130 K, with refinement at $R1 = 0.088$, the displacements of the β and *meso* carbons are 1.02 Å and 0.00 Å, respectively. We consider the conformations of the two crystal forms to be equivalent given the small differences (for nonplanar porphyrins) in out-of-plane displacements between them. Therefore, data for the second crystal form are only reported in the Supporting Information.

Unlike the comparable excursions from planarity in the two crystal forms of ZnDPP described above, significantly different conformations are adopted by H_2DPP in different space groups. An earlier structure of $\text{H}_2\text{DPP}\cdot 3\text{CH}_2\text{Cl}_2$ at 130 K in space group *Cmc2₁* revealed^{4a} an unusual, uneven saddle conformation with one set of opposite pyrrole rings markedly more displaced out-of-plane than the other, see Figure 2. Crystallization of H_2DPP from wet alcoholic KOH yields $\text{H}_2\text{DPP}\cdot 3\text{H}_2\text{O}$ in space group *Pnma* and a new spatial arrangement for the porphyrin. Numerical comparisons of the deviations from planarity in the two conformers are made in Figure 2. Note that the H_2DPP structure reported now is much more symmetrical and again approaches a normal but very steep saddle with the average β carbon displacements notably larger than those in the ZnDPP, ~ 1.3 vs ~ 1.0 Å. We attribute this additional flexibility in the free base to the fact that the pyrrole nitrogens are not constrained by the bonds to the Zn which tend to limit the out-of-plane tilt of the pyrrole rings. The two H_2DPP structures certainly illustrate the rather wide range of structural excursions or “surfing” possible for the same molecule, and the combined results for the Zn and H_2DPP s document the conformations accessible for the same macrocycle within the generic class of saddle conformations.

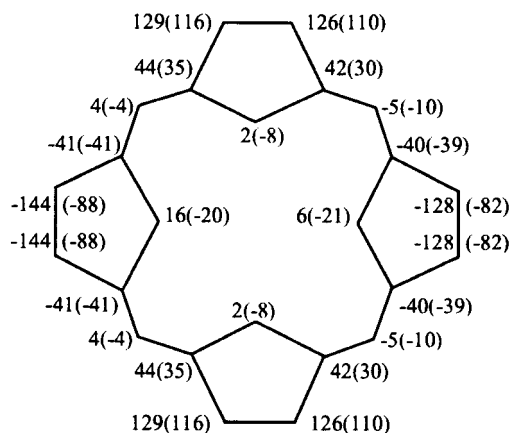


Figure 2. Deviations from planarity, in units of 0.01 Å, for the H₂-DPP described here and, in parentheses, for the conformer reported previously.^{4a} (Esds ~0.01–0.02 Å).

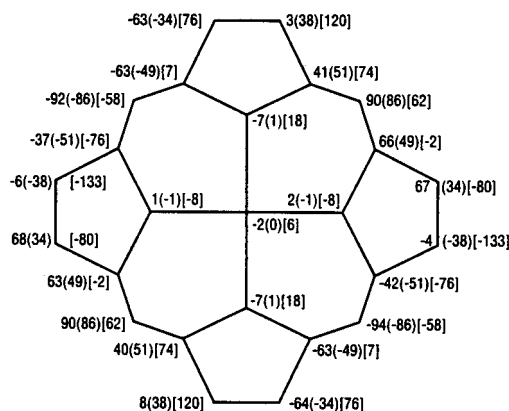


Figure 3. Deviations from planarity, in units of 0.01 Å, in three conformers of NiDPP. From left to right: the asymmetric ruffled structure, **2**. In parentheses: the symmetrically ruffled structure **1** reported previously.^{4b} In brackets: the structure with a combination of ruffled and saddled distortions, **3**.

Low spin Ni(II) porphyrins and hydroporphyrins have provided some of the earliest and best examples of conformational distortions and polymorphism in porphyrin chemistry.^{3d,11,18} This ability to adopt multiple conformations has also been established in solution by resonance Raman⁴ and extended X-ray absorption fine structure (EXAFS)^{3d} spectroscopies. As the macrocycles deviate from planarity, the pyrrole nitrogens move closer to the small Ni(II) ion and the Ni–N distances shorten from ~1.96 Å to ~1.90 Å or less.^{3d,11,18} Although these differences may seem small, short Ni–N distances have become reliable reporters of macrocycle distortions in *low-spin* Ni(II) porphyrins. An EXAFS study of NiDPP yielded^{3d} Ni–N values of 1.88 Å in toluene and 1.91 Å in powders, clearly indicative of a nonplanar conformation. Molecular mechanics (MM) calculations predicted^{4a} the lowest energy conformer to be saddle-shaped with Ni–N = 1.915 Å. A recent crystallographic study of NiDPP(**1**) in space group $F\bar{4}3c$, with six molecules of cyclohexane and one of chloroform per porphyrin occluded in the crystal lattice, yielded^{4b} a Ni–N distance of 1.909(5) Å in good agreement with the powder EXAFS results and the MM calculation, but unexpectedly, the molecule assumed a symmetrical, well-defined ruffled distortion; see the numbers in parentheses for each skeletal atom in Figure 3.

Further dramatic examples of the conformational plasticity of the DPP macrocycle are provided by the two new NiDPP structures presented here. One of these (**2**) crystallizes with 3.5 chloroforms of solvation in space group $P2_12_12_1$ with a

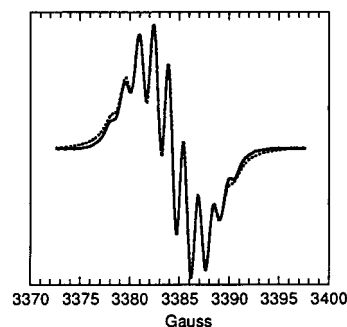


Figure 4. EPR spectrum of ZnDPP⁺·ClO₄[−] in CH₂Cl₂ at RT(—), and a simulation which assumes that 4 equivalent nitrogens ($a_N = 1.43$ G, line width = 1.3 G) determine the major features of the experimental spectrum (---). g -value = 2.0027.

significantly different ruffled distortion than that observed for **1** above. The β carbons of the pyrroles move asymmetrically out-of-plane: in each ring, one β carbon is displaced by ~0.7 Å, while its vicinal neighbor moves less than 0.1 Å. Concomitantly, all the *meso* carbons are displaced by ~0.9 Å; see the first set of values in Figure 3. A second solvate of NiDPP with 1.5 H₂O crystallizes in the same $P2_12_12_1$ group and adopts the same conformation. The number and chemical composition of the solvate molecules thus do not control the conformation of the NiDPP. Here again, the average Ni–N distances are short, 1.894(12) Å.

An additional new form of NiDPP (**3**) crystallizes in space group $C222_1$ without any molecules of solvation. At 200 and 300 K, it adopts a combination of saddled and ruffled distortions with alternate pyrrole rings above and below the mean porphyrin plane but with the rings twisted such that adjacent β carbons are unequally displaced ~0.8 and 1.2–1.3 Å above and below the plane. The *meso* carbons are the least displaced within the three different structures, by ~0.6 Å; see the numbers in brackets in Figure 3.¹⁹ The Ni–N distances of 1.885(6) Å are also marginally the shortest within the series.

These results thus clearly reinforce the empirical rule that short Ni–N distances in low-spin Ni(II) porphyrins faithfully signal the nonplanarity of the complexes. However, they do not discriminate between different types of distortions. Note that these modes are not simply convenient crystallographic descriptors. The majority of *in vivo* distortions observed in porphyrinic protein complexes fall in the ruffled category.^{8–10}

The transient π cation radicals that evolve in photosynthetic and heme-mediated enzymatic electron transfer exhibit distinct unpaired spin density profiles dictated by the symmetry of the HOMO, a_{1u} or a_{2u} (in D_{4h} symmetry).^{6,12–14} The expanding crystallographic evidence for the existence of nonplanar chromophores and prosthetic groups in porphyrin protein complexes thus raises the obvious question as to the effects of macrocycle distortions on the orbital occupancy of π cation radicals.^{6,7} Furthermore, in the numerous synthetic porphyrins designed to mimic biological electron transport and catalysis, the electronic effects of peripheral substituents and their placement at the *meso* and β carbons also need to be considered,^{6,7,12–14} whether or not they induce macrocyclic distortions.

Figure 4 presents the EPR spectrum of the ZnDPP⁺·ClO₄[−] radical. A simulation of the experimental results establishes that the 9-line spectrum arises from four equivalent nitrogens with $a_N = 1.43$ G. This hyperfine pattern closely resembles that of the much simpler ZnTPP⁺·ClO₄[−] and is characteristic of an a_{2u} half-occupied HOMO ($^2A_{2u}$ radical) in which unpaired spin density is concentrated at the nitrogens and *meso* carbons.¹³ (Spin density at the latter is not observed directly in TPPs or

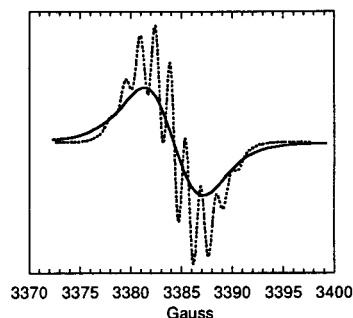


Figure 5. EPR spectra of $\text{ZnDPP}^+\cdot\text{ClO}_4^-$ (---) and $\text{NiDPP}^+\cdot\text{ClO}_4^-$ (—) in CH_2Cl_2 . The Ni radical has a higher g -value of 2.0068, and its spectrum has been recentered to coincide with that of the Zn species to facilitate comparison of line widths.

DPPs because the phenyl groups are oriented out of the porphyrin planes. Spin density at the phenyl protons does contribute to the individual line widths of the observed nine-line spectra.¹³ The EPR spectrum of $\text{NiDPP}^+\cdot\text{ClO}_4^-$ is shown in Figure 5. Although its spectrum is unresolved, comparison of its line width ($\Delta H = 5.9$ G) with that of $\text{ZnDPP}^+\cdot$ indicates that $\text{NiDPP}^+\cdot$ is also a $^2\text{A}_{2u}$ radical.^{20,21} Occupancy of the a_{1u} HOMO or significant mixing of the a_{1u} and a_{2u} orbitals would yield a much narrower line width because the a_{1u} orbital localizes unpaired spin density at the α and β carbons of the pyrrole rings.¹³ The EPR results for the DPP radicals support our previous observations⁷ that macrocycle distortions alone do not switch the HOMO occupancy of porphyrin π cation radicals from a_{2u} to a_{1u} .²¹ Nonetheless, the observed spin profiles of the DPP radicals obviously reflect the combined effects of the conformational distortions and those of the 12 peripheral phenyl rings.

Conclusions

The three different NiDPP structures discussed above represent an unprecedented wide range of conformational excursions for a single porphyrin molecule. In combination with the ZnDPP and H_2DPP results, they illustrate the remarkable plasticity and striking multitude of landscapes accessible within a family of compounds with the exact same peripheral substituents. These ground state results certainly support the conclusions reached from the excited-state dynamics of DPPs¹ and other sterically encumbered porphyrins² that multiconformational landscapes of the types previewed here also evolve in excited states and thus facilitate curve crossing and deactivation to the ground state. Our observations that skeletal distortions can shorten excited-state lifetimes of porphyrins by orders of magnitude² suggest that such distortions play an important role in controlling the photophysics and chemistry of the nonplanar chromophores increasingly evident in crystal structures of photosynthetic antenna and reaction center protein complexes.⁸ Furthermore, the demonstrated acute sensitivity of porphyrin properties^{1–7} to structural motifs found in photosynthetic and heme proteins^{8–10} should lead to new classes of synthetic porphyrins conformationally tailored to exhibit specific ground and excited-state properties.

Acknowledgment. We thank Dr. Jonathan C. Hanson for his assistance with the data acquired at the NSLS. This work was supported by the Division of Chemical Sciences, U.S. Department of Energy, under Contract DE-AC-02-76CH00016, at Brookhaven National Laboratory and by National Science Foundation Grant CHE-96-23117 at the University of California.

Supporting Information Available: Listings of experimental crystallographic details, atomic coordinates, bond distances, and bond angles for $\text{ZnDPP}\cdot 3.5\text{C}_6\text{HCl}_3$, $\text{ZnDPP}\cdot 5\text{C}_6\text{H}_{12}$, $\text{H}_2\text{DPP}\cdot 3\text{H}_2\text{O}$, NiDPP, NiDPP $\cdot 3.5\text{CHCl}_3$, and NiDPP $\cdot 1.5\text{H}_2\text{O}$ (62 pages). Ordering information is given on any current masthead page.

References and Notes

- (1) (a) Gentemann, S.; Nelson, N. Y.; Jaquinod, L.; Nurco, D. J.; Leung, S. H.; Medforth, C. J.; Smith, K. M.; Fajer, J.; Holten, D. *J. Phys. Chem. B* **1997**, *101*, 1247. (b) Drain, C. M.; Kirmaier, C.; Medforth, C. J.; Nurco, D. J.; Smith, K. M.; Holten, D. *J. Phys. Chem.* **1996**, *100*, 11984.
- (2) Gentemann, S.; Leung, S. H.; Smith, K. M.; Fajer, J.; Holten, D. *J. Phys. Chem.* **1995**, *99*, 4330. Gentemann, S.; Medforth, C. J.; Ema, T.; Nelson, N. Y.; Smith, K. M.; Fajer, J.; Holten, D. *Chem. Phys. Lett.* **1995**, *245*, 441. Gentemann, S.; Medforth, C. J.; Forsyth, T. P.; Nurco, D. J.; Smith, K. M.; Fajer, J.; Holten, D. *J. Am. Chem. Soc.* **1994**, *116*, 7363. Regev, A.; Galili, T.; Medforth, C. J.; Smith, K. M.; Barkigia, K. M.; Fajer, J.; Levanon, H. *J. Phys. Chem.* **1994**, *98*, 2520.
- (3) (a) Renner, M. W.; Barkigia, K. M.; Fajer, J. *Inorg. Chim. Acta* **1997**, *263*, 181. (b) Ozette, K.; Leduc, P.; Palacio, M.; Bartoli, J.-F.; Barkigia, K. M.; Fajer, J.; Battioni, P.; Mansuy, D. *J. Am. Chem. Soc.* **1997**, *119*, 6442. (c) Renner, M. W.; Barkigia, K. M.; Melamed, D.; Smith, K. M.; Fajer, J. *Inorg. Chem.* **1996**, *35*, 5120. (d) Renner, M. W.; Barkigia, K. M.; Zhang, Y.; Medforth, C. J.; Smith, K. M.; Fajer, J. *J. Am. Chem. Soc.* **1994**, *116*, 8582. (e) Ochsenbein, P.; Ayougou, K.; Mandon, D.; Fischer, J.; Weiss, R.; Austin, R. N.; Jayaraj, K.; Gold, A.; Terner, J.; Fajer, J. *Angew. Chem., Int. Ed. Engl.* **1994**, *33*, 348. (f) Barkigia, K. M.; Renner, M. W.; Furenli, L. R.; Medforth, C. J.; Smith, K. M.; Fajer, J. *J. Am. Chem. Soc.* **1993**, *115*, 3627.
- (4) (a) Medforth, C. J.; Senge, M. O.; Smith, K. M.; Sparks, L. D.; Shelnutt, J. A. *J. Am. Chem. Soc.* **1992**, *114*, 9859. (b) Nurco, D. J.; Medforth, C. J.; Forsyth, T. P.; Olmstead, M. M.; Smith, K. M. *J. Am. Chem. Soc.* **1996**, *118*, 10918.
- (5) Takedo, J.; Sato, M. *Chem. Lett.* **1995**, 939.
- (6) Lin, C. Y.; Hu, S.; Rush, T.; Spiro, T. G. *J. Am. Chem. Soc.* **1996**, *118*, 9452. Sibilia, S. A.; Hu, S.; Piffat, C.; Melamed, D.; Spiro, T. G. *Inorg. Chem.* **1997**, *36*, 1013.
- (7) Renner, M. W.; Cheng, R. J.; Chang, C. K.; Fajer, J. *J. Phys. Chem.* **1990**, *94*, 8508. Forman, A.; Renner, M. W.; Fujita, E.; Barkigia, K. M.; Evans, M. C. W.; Smith, K. M.; Fajer, J. *Isr. J. Chem.* **1989**, *29*, 57.
- (8) Prince, S. M.; Papiz, M. Z.; Freer, A. A.; McDermott, G.; Hawthorthwaite-Lawless, A. M.; Cogdell, R. J.; Isaacs, N. W. *J. Mol. Biol.* **1997**, *268*, 412. Ermler, V.; Fritsch, G.; Buchanan, S. K.; Michel, H. *Structure* **1994**, *2*, 925. Deisenhofer, J.; Epp, O.; Sinning, I.; Michel, H. *J. Mol. Biol.* **1995**, *246*, 429.
- (9) Sundaramoorthy, M.; Kishi, K.; Gold, M. H.; Poulos, T. L. *J. Biol. Chem.* **1994**, *269*, 32759. Ravichandran, K. G.; Boddupalli, S. S.; Hasemann, C. A.; Peterson, J. A.; Deisenhofer, J. *Science* **1993**, *261*, 731. Crane, B. R.; Siegel, L. M.; Getzoff, E. D. *Science* **1995**, *270*, 59.
- (10) For an extensive discussion of distortion modes and their associated energies as well as additional references to in vivo distortions, see: Jentzen, W.; Song, X. Z.; Shelnutt, J. A. *J. Phys. Chem. B* **1997**, *101*, 1684.
- (11) The nomenclature is that suggested by Scheidt and Lee (Scheidt, W. R.; Lee, Y. J. *Struct. Bonding (Berlin)* **1987**, *64*, 1). In a saddle conformation, alternate pyrrole rings are tilted up and down with respect to a plane through the 24 atoms of the porphyrin core, and the *meso* atoms lie in that plane. In a ruffled conformation, alternate pyrrole rings are twisted clockwise or anticlockwise about the metal–nitrogen bonds, and the *meso* carbons sit alternately above or below the 24-atom plane.
- (12) Skillman, A. G.; Collins, J. R.; Loew, G. H. *J. Am. Chem. Soc.* **1992**, *114*, 9538. Fujii, H. *J. Am. Chem. Soc.* **1993**, *115*, 4641. Ayougou, K.; Mandon, D.; Fischer, J.; Weiss, R.; Muther, M.; Schünemann, V.; Trautwein, A. X.; Bill, E.; Terner, J.; Jayaraj, K.; Gold, A.; Austin, R. N. *Chem. Eur. J.* **1996**, *2*, 1159.
- (13) Fajer, J.; Davis, M. S. *The Porphyrins*; Dolphin, D., Ed.; Academic Press: New York, 1979; Vol. IV, p 197. Hanson, L. K.; Chang, C. K.; Davis, M. S.; Fajer, J. *J. Am. Chem. Soc.* **1981**, *103*, 663.
- (14) Weiss, R.; Mandon, D.; Wolter, T.; Trautwein, A. X.; Muther, M.; Bill, E.; Gold, A.; Jayaraj, K.; Terner, J. *J. Biol. Chem.* **1996**, *271*, 377. Dolphin, D.; Forman, A.; Borg, D. C.; Fajer, J.; Felton, R. H. *Proc. Natl. Acad. Sci. U.S.A.* **1971**, *68*, 614. Sono, M.; Roach, M. P.; Coulter, E. D.; Dawson, J. H. *Chem. Rev. (Washington, D.C.)* **1996**, *96*, 2841. Dolphin, D.; Traylor, T. G.; Xie, L. Y. *Acc. Chem. Res.* **1997**, *30*, 251.
- (15) Crystallographic results for several Ni(II) and Cu(II) π cation radicals of nonplanar porphyrins show the radicals to be as distorted as the neutral parents.^{3a,c,d}
- (16) Medforth, C. J.; Berber, M. D.; Smith, K. M.; Shelnutt, J. A. *Tetrahedron Lett.* **1990**, *26*, 3719.

(17) Gray, M. J.; Jasper, J. D.; Wilkinson, A. P.; Hanson, J. C. *Chem. Mater.* **1997**, 9, 976.

(18) Meyer, E. F., Jr. *Acta Crystallogr., Sect. B* **1974**, B29, 2162. Cullen, D. L.; Meyer, E. F., Jr. *J. Am. Chem. Soc.* **1974**, 96, 2095. Brennan, T. D.; Scheidt, W. R.; Shelnut, J. A. *J. Am. Chem. Soc.* **1988**, 110, 3919. Kratky, C.; Waditschatka, R.; Angst, C.; Johansen, J. E.; Plaquevent, J. C.; Schreiber, J.; Eschenmoser, A. *Helv. Chim. Acta* **1985**, 68, 1312. Mandon, D.; Ochsenbein, P.; Fischer, J.; Weiss, R.; Jayaraj, K.; Austin, R. N.; Gold, A.; White, P. S.; Brigaud, O.; Battioni, P.; Mansuy, D. *Inorg. Chem.* **1992**, 31, 2044. Suh, M. P.; Swepston, P. M.; Ibers, J. A. *J. Am. Chem. Soc.* **1984**, 106, 6, 5164. Stolzenberg, A. M.; Glazer, P. A.; Foxmann, B. M. *Inorg. Chem.* **1986**, 25, 983.

(19) In all the DPPs discussed here, there exist two types of interactions between the peripheral phenyl substituents. The average distances between the centers of the *meso* phenyls and their flanking β neighbors range between 3.5 and 3.9 Å with most at 3.6–3.7 Å, indicative of weak π – π interactions. In contrast, the center-to-center distances between adjacent β phenyls range between 4.3 and 4.7 Å.

(20) The higher g -value of 2.0068 for NiDPP⁺⁺ compared to that of 2.0027 for ZnDPP⁺⁺ suggests some interactions between the π radical and Ni orbitals which may arise from the shorter Ni–N bond distances.

(21) Although these results are most consistent with a_{2u} orbital occupancies, they do not exclude *some* mixing with the a_{1u} orbital.